

## Résumé

**Wound healing** is important not only for its obvious biological role, but also for the study of tissue growing, collective cell migration and the cell-to-cell feedback process, tumor growth.

**Our motivation** came from a wound healing *in vitro* experiment - by Vedula et al 2011 (fig. 1) - where it was shown that different types of geometric confinement induce cells emergent movement into distinct migration patterns.

**We used** an active matter model (fig. 2) to simulate an *in silico* version of Vedula's experiment with the **objective** to understand further the response of collective movement to this kind of geometrical boundaries.

**We show**, along with other results, that the shape of the reservoir - where cells are migrating from - also define emerging patterns as to those found experimentally *in vitro*, associated before only to the tracks widths (figs 6,7,8).

**This detail** was not mentioned in the experimental result, but resulted to be important in the simulations. Hence, within the limits of the active matter approach followed here, **we conclude** that the **shape and size** of the reservoir are **fundamental aspects** to be analyzed in future experiments of this nature.

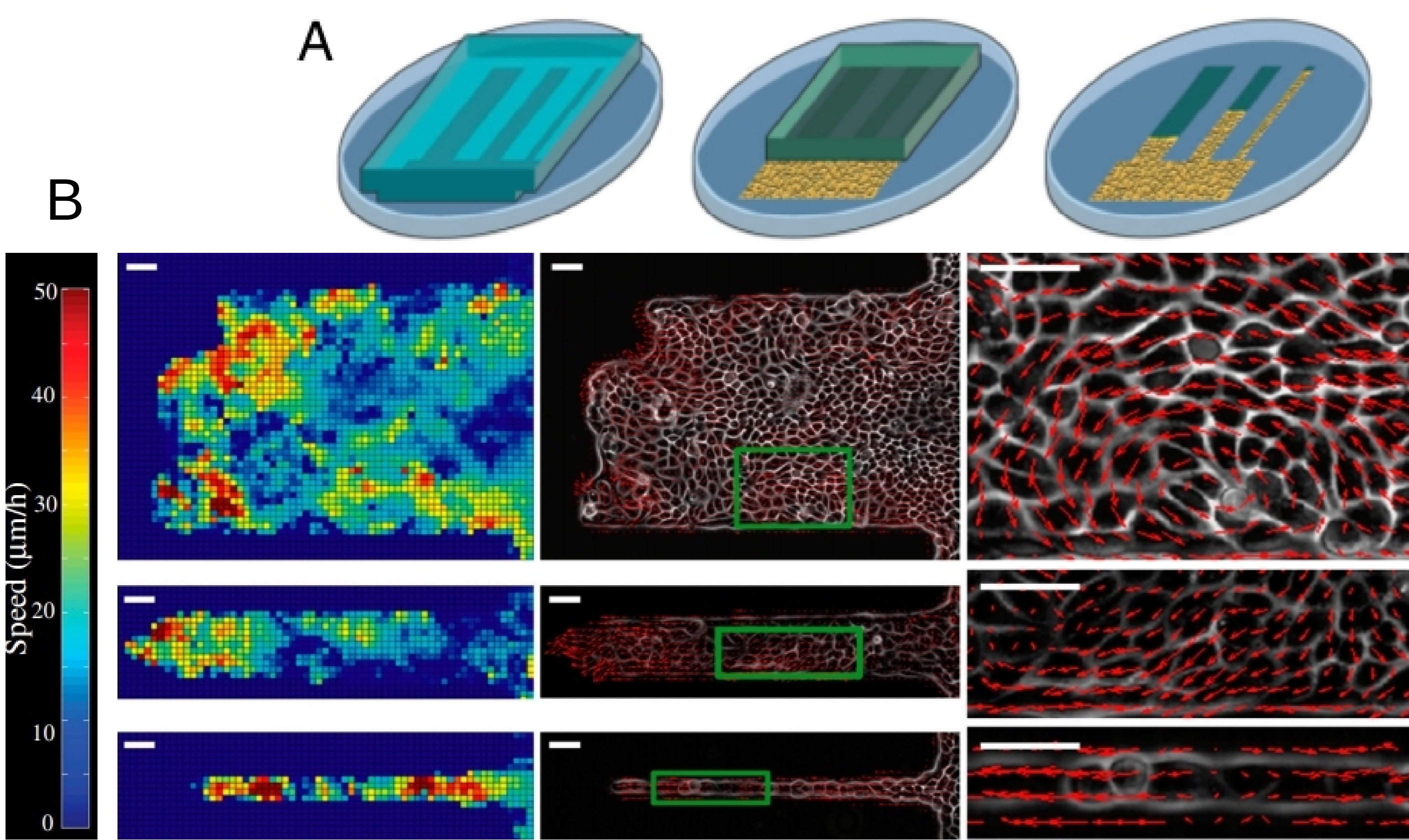


**Fig. 1:** From Vedula et al 2011. (A) *In vitro* experiment sketch: Cells were grown to confluence inside the reservoir and then released to tracks with different widths. (B) Cells velocity image mapping on three distinct tracks width (20, 100 and 400 µm, from top to bottom - 10µm ~ 1 cell diameter). To the left, the heat map where higher velocities are in red and lower velocities in blue. In the center are the vectorial velocity fields. To the right, zoom in the center green marked areas: the caterpillar-like movement on the narrower track (bottom), the vortex pattern on the wider track (top) and a intermediate movement occurring on the medium track.

**Active Matter Model :**

$$\vec{r}_i^{t+1} = \vec{r}_i^t + \vec{v}_i^t dt \quad (1)$$

$$\theta_i^{t+1} = \arg \left[ \alpha \sum_{j \in \text{vizi}} \vec{v}_j^t + \beta \sum_{j \in \text{vizi}} \vec{f}_{ij}^t + \eta \vec{u}_i^t \right] \quad (2)$$

$$\vec{f}_{ij} = \hat{e}_{ij} \begin{cases} 0 & \text{se } r_{ij} > dl \\ (1 - \frac{r_{ij}}{de}) & \text{se } dc < r_{ij} \leq dl \\ 1000 & \text{se } r_{ij} \leq dc \end{cases} \begin{matrix} dl == 0.45 \\ de == 0.40 \\ dc == 0.20 \end{matrix} \quad (3)$$

$$v_{ki}^t = \begin{cases} -rf * |v_{ki}^t| & \text{se } k_i \geq L_k \\ rf * |v_{ki}^t| & \text{se } k_i \leq -L_k \end{cases} \quad (k = x, y \text{ e } rf \in [0, 1.0]) \quad (4)$$

$rf == 0.2$

**Fig. 2:** The three first equations defines a classic polar alignment Vicsek's self propelled particles model (SPPs) with an harmonic radial force. Equation (4) is a attenuated rigid wall boundary condition that plays the hawl of the geometric constrains. A good portion of SPPs models are performed in periodic boundaries, since eq. (4) introduces a still new and not trivial feature to the problem.

## Simulations, discussions and methodology:

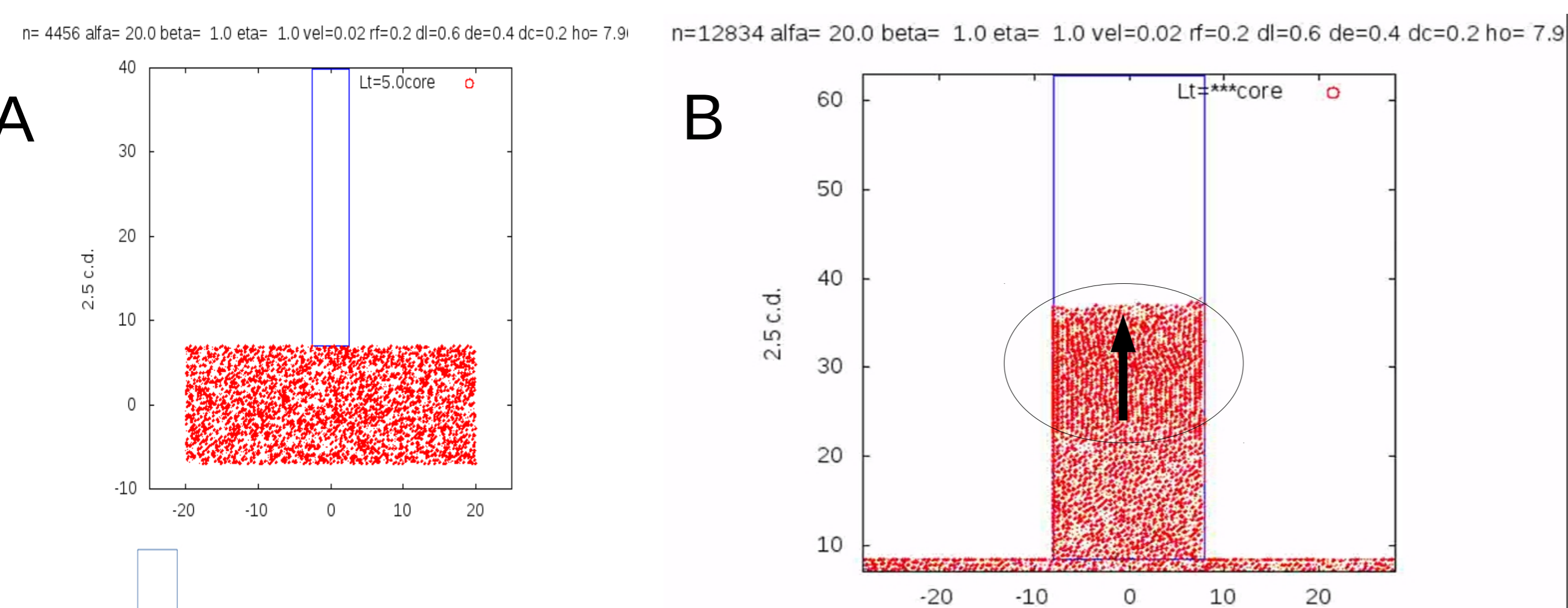


**Fig. 3:** (A) Simulation initial condition: in blue we see the track wall and under it the reservoir full of cells. (B) Wide track: the directed density fluctuations (caterpillar movement) is depicted in the image. This pattern was obtained in all tracks widths. (C) Simple sketch of how the reservoir shape could enhance the inner track movement.

**Fig. 4:** Snapshots of the two simulations types used to investigate how the reservoir rectangular shape can enhance or reduce the inner tracks caterpillar movement. Depicted in both images the directed density fluctuations: (A) Reservoir with large Y direction parallel to the track. (B) Reservoir with large X direction orthogonal to the track.

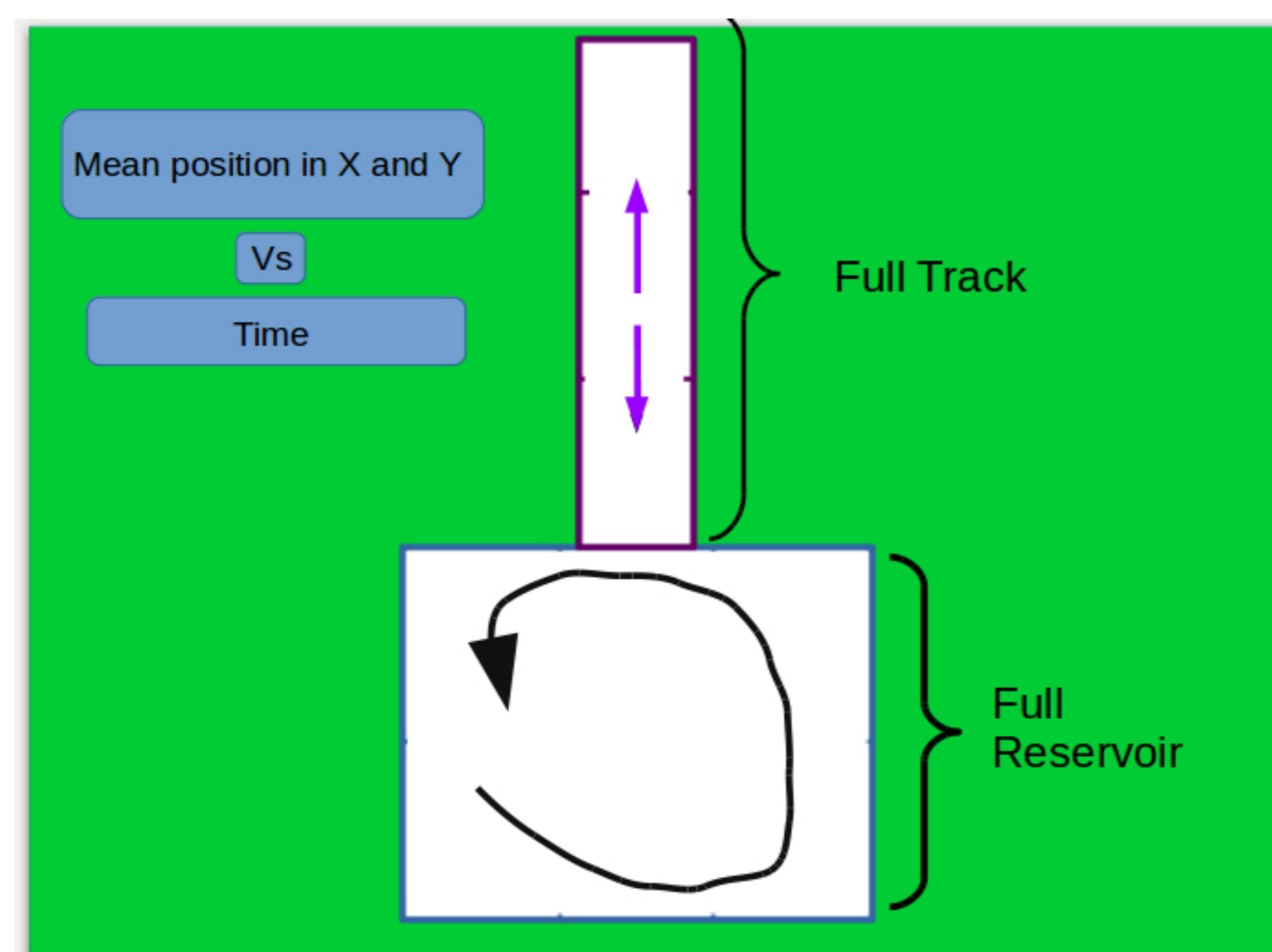
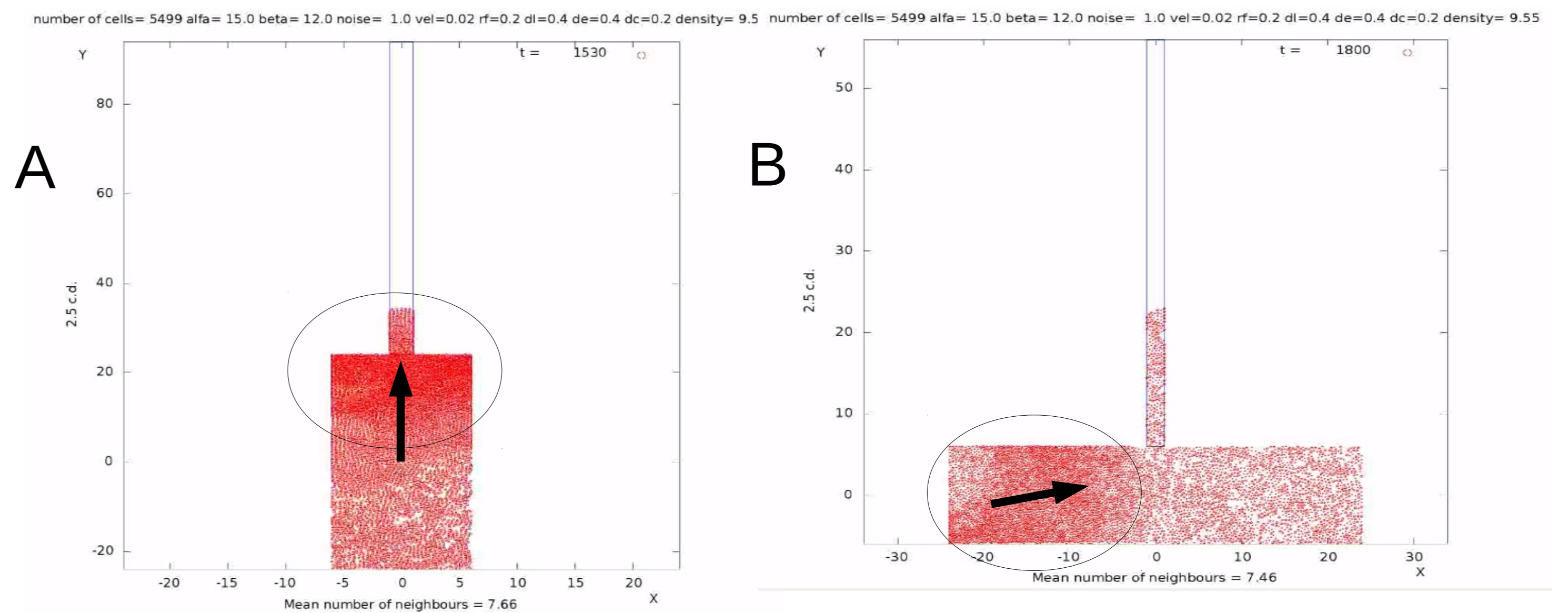
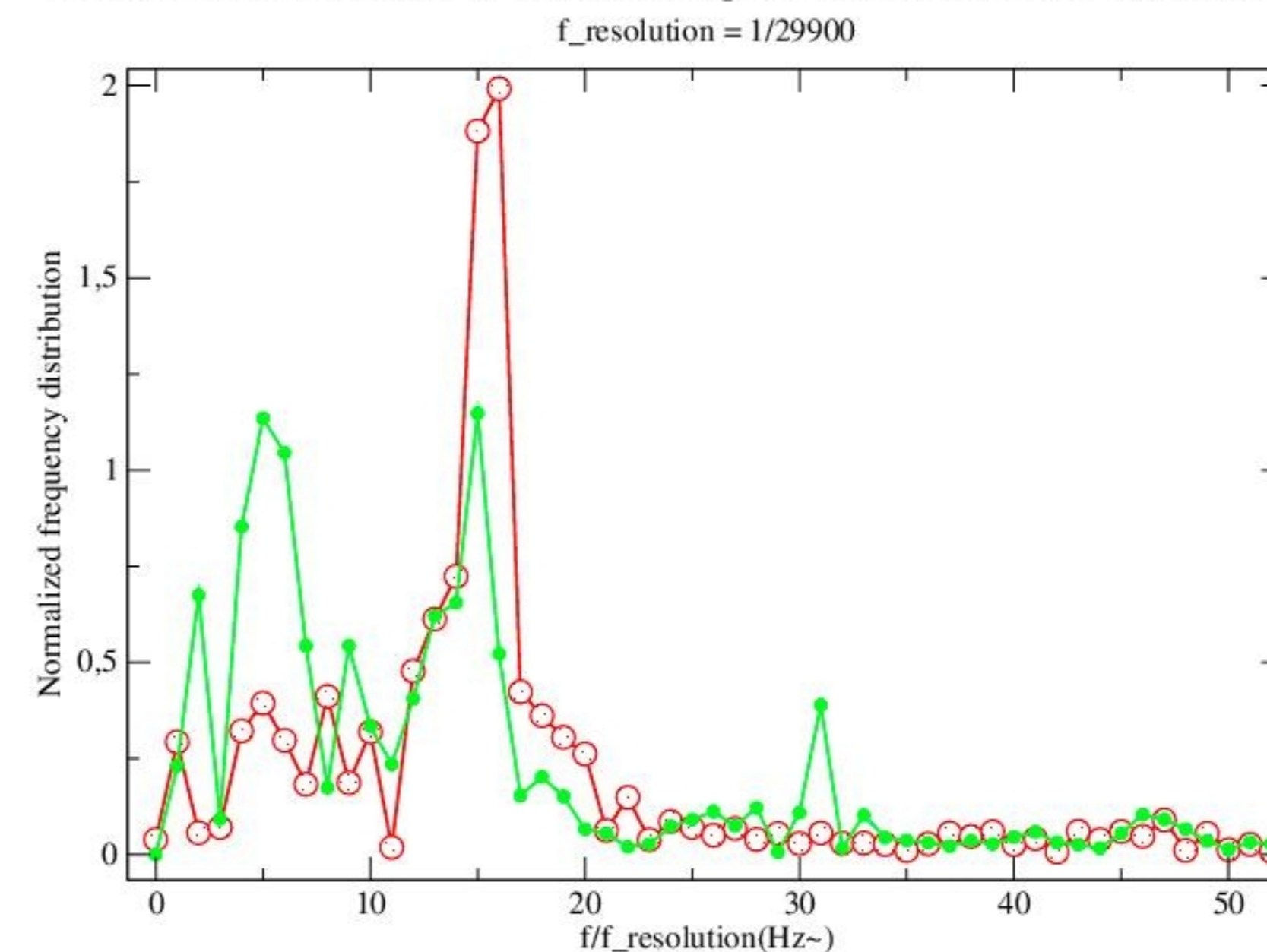


**Fig. 5:** Drawing explaining the method adopted to correlate the oscillations in the reservoir with the oscillations in the track, represented by the black curl and the up and down purple arrows respectively. We measured the mean X and Y position (center of mass) of all the particles inside the reservoir and plotted vs time. We did the same for the particles inside the track and then we compared this two signals (curves).

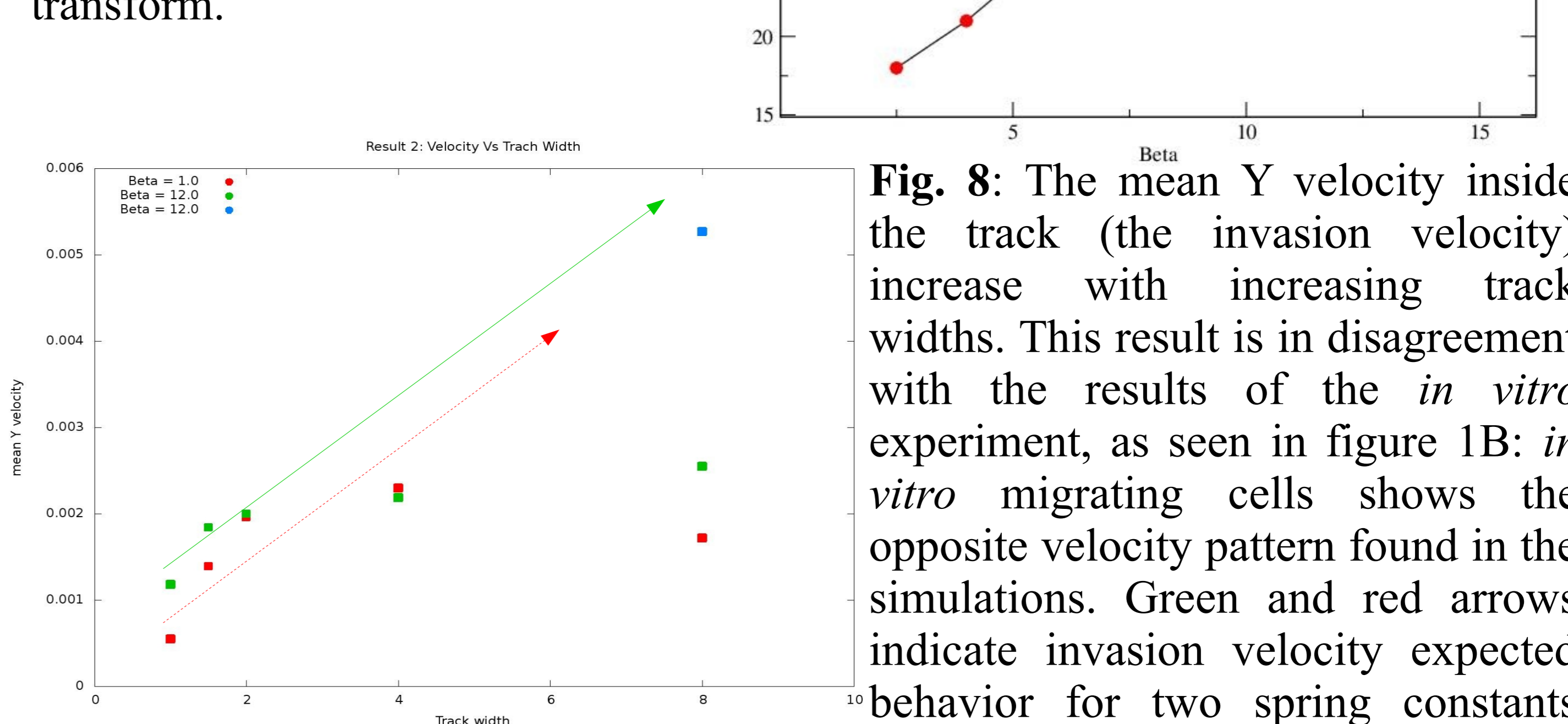
Fourier transform of Y full track (green) and reservoir (red) timbre



**Result:**  
**Fig. 6:** Discrete Fourier transform of the two Y signals discussed in fig. 5 and measured in the simulation showed in fig. 4A. In red we see the frequency distribution in the reservoir and in green the ones for the track. The good agreement with the two curves indicates, as a preliminary result, the correlation between the track/reservoir oscillations.

## Others results:

**Fig. 7:** The most (*Max*) predominant oscillation frequency inside the reservoir grows linearly with increasing spring constant ( $\beta$ ) value. We obtained the *Max* frequencies using the Fourier transform.



## Conclusions:

- Vortices's were obtained in large enough reservoirs, although together with density fluctuations;
- Caterpillar-like movements are obtained due to density fluctuations in the reservoir, present at all types of tracks.
- The mean velocity in the tracks increase with the tracks width and with increasing spring constant ( $\beta$ ) values;
- Reservoir oscillation frequency increase with increasing spring constant ( $\beta$ ) values;
- Reservoir shape determines collective movement in the tracks;

**Fig. 8:** The mean Y velocity inside the track (the invasion velocity) increase with increasing track widths. This result is in disagreement with the results of the *in vitro* experiment, as seen in figure 1B: *in vitro* migrating cells shows the opposite velocity pattern found in the simulations. Green and red arrows indicate invasion velocity expected behavior for two spring constants ( $\beta$ ) values without the reservoir emptying effect.